Automatic Tooth Restoration via Image Warping

Sebastian Meller Matthias Wolf Dietrich Paulus
Matthias Pelka Peter Weierich Heinrich Niemann

Bavarian Research Center for Knowledge Based Systems (FORWISS)
Research Group Knowledge Processing
Am Weichselgarten 7, D-91058 Erlangen, Germany

{*snmeller*|*wolf*}@forwiss.uni-erlangen.de

In: Proc. CAR'97 Berlin
(7 pages)

S. Meller, M. Wolf, M. Pelka, D. Paulus, H. Niemann: *Automatic Tooth Restoration via Image Warping*, in H. Lemke, M. Vannier, K. Inamura (Hrsg.): *Computer Assisted Radiology*, Nr. 1134 in International Congress Series, Berlin, Juni 1997, S. 221–227.
ISBN: 0 444 82756 0

Contents

Automatic Tooth Restoration via Image Warping

Sebastian Meller, Matthias Wolf, Peter Weierich[a] and Matthias Pelka[b] and Dietrich Paulus[c] and Heinrich Niemann[a,c]

[a] Bavarian Research Center for Knowledge Based Systems (FORWISS)
Research Group Knowledge Processing
Am Weichselgarten 7, D-91058 Erlangen, Germany

[b]Policlinic for Restorative Dentistry and Periodontology
Glückstr. 11, D-91054 Erlangen, Germany

[c]Chair for Pattern Recognition (Computer Science 5)
Martensstr. 3, D-91058 Erlangen, Germany

Automatic tooth restoration systems produce dental restorations for individual given teeth with a prepared cavity. Whereas the shape of the inlay inside the tooth is determined by the shape of the cavity the chewing surface yet has to be defined. We present RecOS, a method that makes use of an intact chewing surface of a model tooth to determine the chewing surface of an inlay, onlay or crown to be ground by an NC–machine e.g. from ceramics. The method uses the technique of image deformation to provide a congruence between range images of the model tooth and the prepared tooth such that the missing part is determined by the deformed model tooth. The image deformation is defined by a number of pairs of mutually corresponding feature points in both range images. Feature extraction techniques including active contours [4] are used to detect these points. A new approach for contour–matching is proposed to match corresponding feature points of the two different teeth. Our implementation was tested on a number of range images with manually marked cavities. The mean height difference between the restored surface and the original surface was between 0.2 mm and 1.0 mm. This is only half of the difference measured on machine–made inlays of a commercial system. The method can be extended to consider the chewing surface of antagonistic teeth as well.

1. Introduction

Toothaches are an unwelcome reason to see your dentist. After removing the source of pain, usually caries, the remaining gap has to be filled again. Amalgam – though still favored by a lot of dentists as an excellent filling material – has recently lost its popularity due to its still discussed toxicity. Following the demand for tooth–colored restorations, the market for ceramics as a filling material is currently growing. However, the traditional way of manufacturing inlays from ceramics requires imprints of both jaws which are unpleasant to be taken, at least two visits at the dentist's and the participation of a dental technician to manufacture the inlay in a complicated process involving several steps.

In order to reduce this effort, CIM–systems like the Cerec^{R} system [7] have been developed which allow a computerized interactive construction of ceramic inlays in one appointment. An optical imprint of the prepared tooth is taken intraorally with a specialized camera that produces range images of the tooth surface. Whereas the shape of the inlay inside the cavity can be calculated directly from the range data, the chewing surface is shaped manually in a CAD system on the screen. The inlay can then be ground by an NC–machine from a raw block of ceramics. Usually the produced inlay needs some corrections with a diamond drill to achieve a smooth continuation of the original tooth surface and to fulfill the requirements of the chewing process, which takes precious time and unavoidingly removes healthy substance from the tooth.

Our system aims for the reduction of the required manual contributions in the shaping process. After a survey of the state of the art in this area in Section 2 and a description of the images we use in Section 3 the steps of our method are described. The idea of the RecOS method (Reconstruction of Occlusal Surfaces[1])[6] is to make use of the intact occlusal surface of the model tooth to determine the occlusal surface of an inlay, onlay or crown to be ground by an NC–machine for the given tooth to be restored. In order to do this range images of both teeth are made congruent by an image deformation of the model tooth that is based on extracted feature points as control points. Section 4 describes the detection of these points, Section 5 the matching of corresponding points in both images as a prerequisite of the image deformation in Section 6. After copying the range data into the cavity, a final height adjustment (Section 6) of the inlay surface ensures a smooth transition between inserted and original tooth surface. Some results are discussed in Section 7 and a summary and outlook follow in Section 8.

2. State of the art

Only very few publications deal with the field of automatic tooth restorations. For dental range images, interactive approaches for feature detection are described in [9,11], whereas the automatic method in [15] is only applicable for intact chewing surfaces. Concerning complete systems besides the mentioned Cerec^{R} system [7,8], two patent descriptions [12,1] are available. Both use affine transformations of a 3D model tooth to adapt it to the given tooth and they mainly consider the production of crowns instead of inlays and onlays for a given incomplete tooth surface. In [3] a deformable 3D tooth model is adapted to intact model teeth in an energy minimizing process. It is planned to use this model to restore missing surface parts in the future. The issue of surface representations for tooth models and the conversion into a program for an NC–machine is addressed in [5].

3. Images

The range images we use were taken with a camera from the Cerec^{R} system based on phase–measuring triangulation [2]. A typical example is given in Figure 1a and 1b where range values are coded as gray values. The sensor provides range images with a resolution of 700×480 pixels and 256 possible range values covering 7.3 mm of height with a pixel corresponding to a $30 \times 30\,\mu$m square on the tooth surface.

[1]patent pending

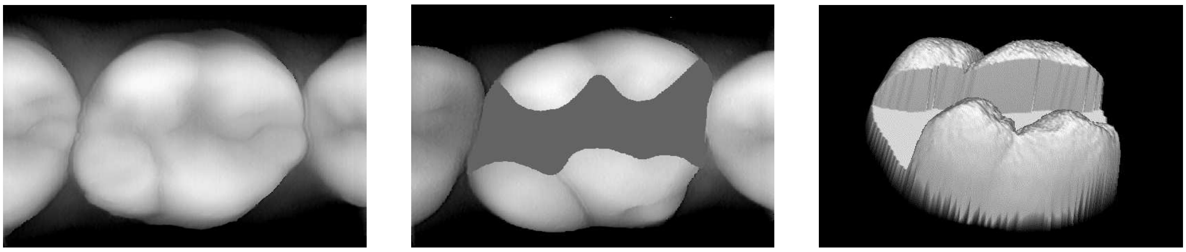

Figure 1. A range image of a model tooth (a), a prepared tooth (b) and its 3D–visualization (c). The cavity was simulated by blacking out an area in the range image in order to enable an evaluation of our reconstruction method.

4. Feature detection

The detection of the outer contour lines of both teeth as one part of the required control points for the image deformation step is performed in two steps. The first step is a rough estimation of the centers and outlines of all teeth in each range image. A ring–shaped mask with diameters to cover the tooth outlines of differently sized teeth is moved across the gradient image of the range image. The sum of the gradient values within the mask is associated with the center pixel. Local maxima in the resulting image of gradient sums represent possible tooth centers. The local maxima are detected with an algorithm similar to the watershed transformation [14]. The method allows to detect even the partly visible neighboring teeth and prepared teeth with a sometimes incomplete outline. The maximum gradient values within the ring mask on rays starting at the detected tooth center points give a rough estimation of the tooth outlines to be refined in the second step. Figure 2a shows the ring mask at the three detected tooth centers with the contour estimation.

The second step uses the active contour or snake approach [4]. In our application we have chosen a number of $N = 200$ control points, also called *snaxels*, to describe the shape of the outer contour line. Initial snaxel positions are defined by the contour estimation from the first step. During the iterative energy minimization process the snaxel positions are changed until the sum of the gradients along the contour is maximized and the local curvature is minimized. Thus it is possible to approximate the tooth outline and to span gaps in the outline of the prepared tooth caused by a cavity. If necessary, larger gaps can be spanned with user support semi–interactively. An example of a detected outline is given in Figure 2b where adjacent snaxels are connected with lines.

After extracting the tooth from the background, characteristic feature points in the occlusal surfaces are detected. Typical features of molars are the number and the positions of the cusp tips as well as the shape of the fissures. Cusp tips are detected as local maxima with the same algorithm described above. Points of the fissure which lie on the intersection of the fissure and a straight connection between two adjacent cusp tips are detected by searching for local minima on these lines. The positions of the inner feature points for a prepared chewing surface are shown in Figure 2c.

5. Feature Matching

The image warping technique we use (see Section 6) is based on pairs of control points, in our case contour and characteristic feature points of the model tooth and their cor-

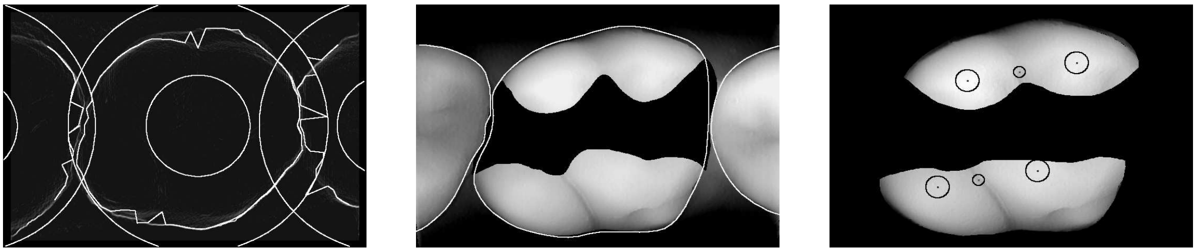

Figure 2. Rough estimation of tooth centers and outlines (a) in the gradient image, the refined contour (b) and characteristic feature points inside the chewing surface (c).

responding points in the prepared tooth. The problem of correspondence is well–known from stereo–vision or detection of motion [10]. Our solution reduces the two–dimensional problem to a one–dimensional matching of the sequences of snaxels obtained from the snake approach of Section 4. The contours of two teeth of the same type (e.g. molars) are similar. This similarity can be described by four criteria which are invariant with respect to scale, translation and rotation. These criteria are determined for each snaxel yielding four sequences of measured data per tooth (Figure 3):

1. The distance r_i from each snaxel to the tooth center M
2. The local curvature ϕ_i at each snaxel $\boldsymbol{P}_i = (x_i, y_i)$, approximated by $\phi_i = \gamma_i - \gamma_{i+1}$ with $\gamma_i = \arctan \frac{y_i - y_{i-1}}{x_i - x_{i-1}}$
3. The distance c_i of each snaxel to the nearest cusp tip
4. The distance f_i of each snaxel to the nearest detected fissure point

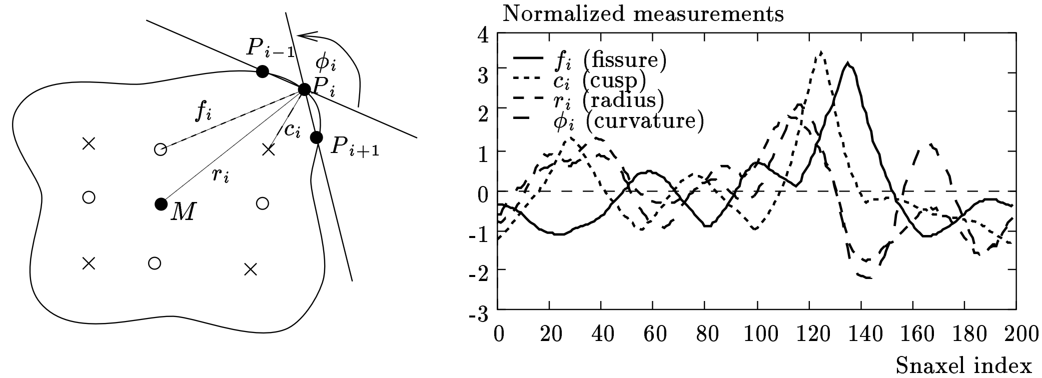

Figure 3. Each snaxel of both teeth is associated with a four–dimensional vector of normalized values. These vectors of both contours are mapped to each other using cross–correlation and "Dynamic Time Warping".

The aim of the matching process is to determine a mapping of the snaxels maximizing a suited measure of similarity for the sequences of measured data for the two teeth. The matching process itself is subdivided into two steps. In the first step, the displacement that maximizes the similarity of the two contour lines is computed by searching for a displacement $j_{max} = \text{argmax}_j \; r_{ab(j)}$, where a and b denote the sequences of measurement vectors $\boldsymbol{a}_i, \boldsymbol{b}_i, i = 1 \ldots N$ of the prepared tooth and the model tooth contour, respectively. The similarity criterion $t_{ab(j)} = \sum_{i=1}^{N} \boldsymbol{a}_i \boldsymbol{b}_{(i+j) \; mod \; N}$ can be interpreted as a vectorial version of the cross–correlation coefficient known from statistics.

In the second step, we apply a method originating from speech recognition, "Dynamic Time Warping" [10], to determine a nonlinear mapping of the contour points. This method minimizes the summed up euclidian distances between measurement vectors of snaxels that are mapped to each other. Minimization over a restricted range of possible mappings is achieved by dynamic programming. A result can be seen in Figure 4 where the model tooth is visualized inside the prepared tooth and corresponding feature points are connected with lines.

Afterwards, the characteristic feature points inside the occlusal surfaces are assigned to each other according to the mapping of the contour points next to them. In case of feature points hidden in the cavity area of the prepared tooth, the assignments are omitted (see also Section 8).

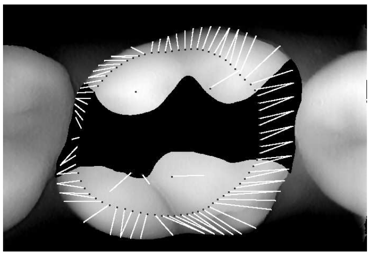

Figure 4. The result of the feature matching process. The inner smaller contour shows the feature points of the model tooth, the outer one belongs to the visible range image of the prepared tooth. Corresponding feature points are connected with lines.

6. Image Warping and Height Adjustment

The pairs of control points can now be used to deform the range image of the model tooth to achieve a congruence of both teeth. A coordinate transformation $\boldsymbol{g} : \boldsymbol{g}(x, y) = (g1(x, y), g2(x, y))$ is performed where $g1$ and $g2$ are calculated as scattered data interpolation functions based on the control points. We use radial base functions known as Hardy's multiquadrics that have proved to be successful for image warping [13]. A resampling of the range image follows. An example of a range image of the deformed model tooth of Figure 1a is shown in Figure 5a. The area in the model tooth corresponding to the cavity can now be copied into the prepared tooth. As positions of cusps and fissures have been made equal in both images by the image deformation, the surface relief of the model tooth is very close to the unknown original one of the prepared tooth. However, an additional height adjustment step is needed, because the image warping did not change the height values of the model tooth. The height difference of the deformed model tooth and the prepared tooth at the cavity edge can be taken as a set of control points for another two–dimensional interpolation. The resulting surface is an estimation of the difference between the surfaces of the deformed model tooth and the unknown original one. Thus the cavity is filled with height values copied from the model tooth added to this estimated difference value at each point. The result is a fully restored occlusal surface with a smooth transition between the restored part and the tooth and a natural continuation of the occlusal relief (Figure 5b). Other methods beyond the focus of this paper can use the calculated surface data to prepare the grinding of the inlay (Figure 5c) or onlay by an NC–machine.

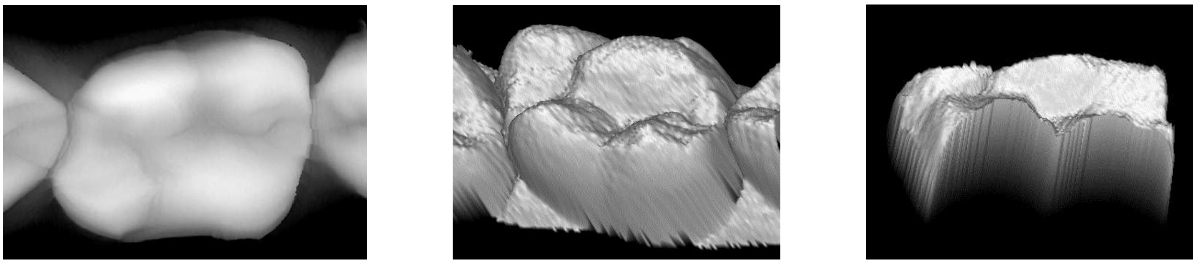

Figure 5. The deformed model tooth (a) (originally Figure 1a), the restored tooth surface (b) and the inlay (c).

7. Results

Our method was implemented in several modules of the Khoros image processing system. In order to evaluate the quality of the achieved results, we have tested our approach with the following experiment: In ten range images a dentist manually blackened appropriate areas in the range images to simulate cavities of three different sizes (see Figure 6). Then a data base of intact model teeth [15], not including the prepared test teeth, was used to reconstruct the destroyed area of the teeth automatically. The data base currently consists of 60 range images of first upper molars of adults. Afterwards the results were compared with the original chewing surface. Depending on the size of the cavity the mean height difference between the reconstructed and the original chewing surface was within a range from 0.2 mm to 1.0 mm. In comparison with the mean height difference measured on Cerec^{R}–inlays [8] the error could be halved.

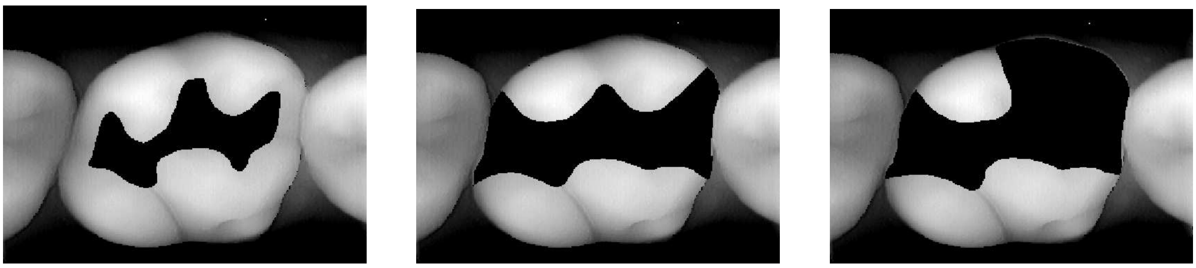

Figure 6. Range images manually marked with differently sized cavities

8. Summary and Outlook

We have presented a new method to determine the shape of a dental restoration for a given prepared posterior tooth. It was tested on a set of range images and showed a high similarity of the restored surface parts with the original tooth surfaces. It also fulfills the dentists' demand for a smooth transition between restoration and tooth and a natural continuation of the occlusal relief.

Until the result of the image deformation highly depends on the number of cusps detected in the chewing surface of the prepared tooth. In case of big cavities some cusps will not be detected and therefore the deformed model tooth may not have the same occlusal relief as the prepared tooth. In these cases optical imprints of the antagonistic teeth of the opposite jaw can provide clues for the missing cusp positions and introduce control points for the height adjustment (Section 6) in order to optimize the role of the restored tooth in the chewing process. This point and the automatic choice of the optimal model tooth for a given tooth will be the goal of further development.

Concerning the ongoing process of automization in this area we hope that future developments will still respect the experience of human experts and may lead to lower costs for dental restorations and thus enable more people to improved dental care.

REFERENCES

1. F. Duret. Method of making a prosthesis, especially a dental prosthesis. Technical report, United States Patent Nr. 4742464, 1988.
2. M. Gruber and G. Häusler. Simple, robust and accurate phase-measuring triangulation. *Angewandte Optik*, 89(3):118 – 122, 1992.
3. S. Gürke. Modellbasierte Rekonstruktion von Zähnen aus intraoralen Tiefenbildern. In B. Arnolds et al., editor, *Digitale Bildverarbeitung in der Medizin*, Freiburg, 1997.
4. M. Kass, A. Witkin, and D. Terzopoulos. Snakes: Active contour models. In *Proc. First Int. Conf. on Computer Vision (ICCV)*, pages 259–268, London, 1987.
5. S. Küppers. Generierung eines 3D-Zahnmodells aus 2,5D-Sensordaten. Technical report, Diploma thesis, University of Erlangen-Nuremberg, Erlangen, 1995.
6. S. Meller. Rekonstruktion von Zahnoberflächen mittels Bilddeformationsmethoden. Technical report, Studienarbeit, University of Erlangen-Nuremberg, Erlangen, 1996.
7. W. H. Mörmann and M. Brandestini. *Die CEREC Computer Reconstruction.* Quintessenz-Verlag, 1989.
8. W. H. Mörmann and A. Mattiola. Computer-generated occlusion of cerec2 inlays and onlays. In *CAD/CIM in aesthetic dentistry.* Quintessence Publishing Co, Inc, 1996.
9. P. J. Neugebauer. Interactive Segmentation of Dentistry Range Images in CIM Systems for the Construction of Ceramic Inlays using Edge Tracing. In *Proceedings of the Computer Assisted Radiology CAR'95 Conference*, 1995.
10. H. Niemann. *Pattern analysis and understanding.* Springer-Verlag, Berlin, Heidelberg, New York, 2 edition, 1990.
11. T. Ozaki, E. Kanazawa, M. Sekikawa, and J. Akai. Three–dimensional measurements of the occlusal surface of the upper molars in australian aboriginals. *Australian Dental Journal*, 32(4):263–9, 1987.
12. D. Rekow. Method and apparatus for modeling a dental prosthesis. Technical report, United States Patent Nr. 5273429, 1993.
13. D. Ruprecht and H. Müller. Free form deformation with scattered data interpolation methods. In G. Farin, editor, *Geometric Modelling (Computing Supplement 8)*, pages 267–281. Springer Verlag, Wien, 1993.
14. L. Vincent and P. Soille. Watersheds in Digital Spaces: An Efficient Algorithm Based on Immersion Simulations. *IEEE Transactions on Pattern Analysis and Machine Intelligence (PAMI)*, 15(6):583–598, 1991.
15. M. Wolf, D.W.R. Paulus, and H. Niemann. Automatic measurement of cusps in 2.5D dental images. In M. Descour and K. Harding D. Svetkoff, editors, *Three-Dimensional and Unconventional Imaging for Industrial Inspection and Metrology*, pages 321–335, 1996.